J. Appl. Comput. Mech., 5(5) (2019) 989-997
DOI: 10.22055/JACM.2019.28640.1496

ISSN: 2383-4536
jacm.scu.ac.ir

M&MoCS
Shahid Chamran University of Ahvaz
Journal of Applied and Computational Mechanics

Research Paper

Finite Integral Transform Based Solution of Second Grade Fluid Flow between Two Parallel Plates

Jaideep Dutta[1], Balaram Kundu[2]

[1] Research Scholar, Department of Mechanical Engineering, Jadavpur University
Kolkata, 700032, India, Email: jdutta.mech@gmail.com

[2] Professor, Department of Mechanical Engineering, Jadavpur University
Kolkata, 700032, India, Email: bkundu@mech.net.in

Received February 17 2019; Revised March 23 2019; Accepted for publication April 09 2019.
Corresponding author: B. Kundu, bkundu@mech.net.in

Abstract. The importance of the slip flow over the no-slip condition is widely accepted in microscopic scaled domains with the direct impact on microfluidic and nanofluidic systems. The popular Navier Stoke's (N-S) flow model is largely utilized with the slip flow phenomenon. In the present study, the finite integral transform scheme along with the shift of variables is implemented to solve the equation of motion of second grade fluid having third-order mixed partial derivative term. The velocity over the flow regime is studied with both the slip and no-slip boundary conditions for Newtonian and non-Newtonian characteristics by considering the generalized Couette flow. The impact of the pressure gradient and flow time on the velocity is investigated analytically. The output of the present work reveals that due to the slip flow velocity randomly varies at the vicinity of wall surface and such nature hasn't been found for the no-slip condition. The validation of the present work was done by comparison with the published work and the numerical values, and it shows well verified.

Keywords: Second grade fluid; Exact solution; Couette flow; Slip condition; Non-Newtonian fluid.

1. Introduction

The present scenario of the research work on flow properties of non-Newtonian fluids attracts the researchers due to its enormous engineering applications such as bio-fluid mechanics, bio-medical engineering, food processing, chemical products extraction, and so on. The engineering materials such as polymer melt, clay coatings and many other emulsions are considered as non-Newtonian fluids [1].

To investigate the unsteady flow regime of non-Newtonian fluids in a specified domain, the major challenge is to choose the correct governing differential equation which can be able to characterize all the rheological behavior of the flow. The impact of slip and no-slip boundary conditions has been forecasted by many researchers. It is well known phenomenon that most of the flow analysis has been carried out in micro scale domain and the postulate of no-slip boundary condition is feasible for very rough boundary surfaces [2]. However, if the boundary surface is very smooth then fluid slips at the boundary interface and no-slip boundary condition is no longer appropriate. Denn [3] studied slip effects on the polymer extrusion process at the boundary in macro domain and witnessed flow instabilities. Further researchers have examined wall slip effects of extrusion [4], experimental effect of slip in PP melt [5] and slip boundary conditions in channel flow [6]. Yang and Zhu [7] developed an analytical solution of squeeze flow of Bingham fluids with Navier slip condition. Erdoğan and İmrak [8] established an exact solution of unsteady unidirectional flow of second grade fluid for Poiseuille flow and generalized Couette flow with no-slip boundary conditions. Wu et al. [9] derived an analytical solution of pressure driven unsteady flow of non-Newtonian fluid in micro-tubes with slip condition. Chen and Zhu [10] evolved the exact solution of Couette–Poiseuille flow of Bingham fluids

Published online: June 14 2019

between two porous parallel plates with a slip effect. Chatzimina et al. [11] mathematically constructed an annular Poiseuille flow for different slip models. Ellahi et al. [12] generated an exact solution of generalized Couette flow with the consideration of non-linear slip. Hady et al. [13] represented the impact of yield stress on free convection layer in non-Newtonian flow over a vertical flat plate embedded in a porous medium filled with nanofluid. Svetlana and Clinton [14] mathematically studied asthenospheric shear in Poiseuillie flow. Jeong [15] numerically simulated the slip effects on rarefied gas flow in micro systems in 2-D and 3-D manner. Noor et al. [16] investigated mixed convection stagnation flow of micropolar nanofluid along a vertical stretching surface with the consideration of slip velocity by implementing shooting method. Sankar and Lee [17] obtained analytical solutions of Herschel-Bulkley fluid in basic different flows with non-linear boundary value problems. Wang et al. [18] analytically and numerically studied unsteady electro-osmotic slip flow of fractional second grade fluid. Ramesh and Sharma [19] developed an approximate analytical solution of magnetohydrodynamic Carreau fluid with boundary conditions in fundamental flows.

The existing research work indicates that in many instances fluid flow is much slower in nature in viewpoint of visco-elastic observation and in such cases second order fluid experiences better characteristic behavior [20]. Based on the literature survey [3-19] illustrated in the above, it has been observed that the fundamental analysis of flow phenomena of no-slip behavior in non-Newtonian fluid flow is not properly focused by the researchers in view point of the second grade fluid flow. Based on such fundamental research gap, the present work is dedicated to analyze Navier linear slip flow characteristics in second grade fluids under the *unsteady condition* and our literature review notifies that the existence of such investigation on unsteady motion is rarely available. The governing differential equation of second grade fluid motion is complex due to presence of 3rd order mixed partial derivative (higher order Navier-Stokes equation). In such cases implementation of finite integral transform (FIT) would be very useful than other solution methods as this technique is particularly suitable for solving higher order partial differential equations [21]. The literature review also indicates that there is no work available in the existing literature base on FIT approach to analyze the second grade fluid flow. Hence the novelty of this research paper is to highlight the ability of FIT scheme to tackle such higher order mixed partial differential equations for both the slip and no slip boundary conditions. The flow velocity in a generalized Couette flow is characterized for Newtonian as well as non-Newtonian fluid. The impact of the unsteady motion has been studied as a function of slip factor and non-Newtonian parameter, and the variation of flow velocity has been experienced for slip and non-slip conditions. Finally, we have authenticated our research work with the published research paper and numerical work developed, and it confirms the exactness of our mathematical formulation as well as computer codes.

2. Mathematical Development

2.1. Governing differential equation for second grade fluid

Based on the theory of continuum mechanics, a very essential model is the second grade fluid flow. The constitutive relation for the second grade fluid model can be written as follows [22]:

$$\sigma = -pI + \mu A_1 + \alpha_1 A_2 + \alpha_2 A_1^2 \tag{1}$$

where, μ, α_1 and α_2 are material moduli and A_n represents the Rivlin-Ericksen tensor defined as follows [22]:

$$A_0 = I, \quad A_1 = \nabla u + (\nabla u)^T, \quad \cdots, \quad A_{n+1} = \left(\frac{\partial}{\partial t} + u.\nabla\right)A_n + (\nabla u)A_n + \left[(\nabla u)A_n\right]^T \tag{2}$$

For unsteady unidirectional flow, the flow field can be approximated as:

$$u = u(y,t); \quad v = 0; \text{ and } \quad w = 0 \tag{3}$$

Using Eq. (3), Eq. (1) can be reformed as:

$$\rho\left(\frac{\partial u}{\partial t}\right) = -\left(\frac{\partial p}{\partial x}\right) + \left(\frac{\partial \sigma_{xy}}{\partial y}\right) \tag{4}$$

where

$$\sigma_{xy} = \mu\left(\frac{\partial u}{\partial y}\right) + \rho\beta\left(\frac{\partial^2 u}{\partial y \partial t}\right) \quad \text{and} \quad \beta = \frac{\alpha_1}{\rho} \tag{5}$$

Inserting Eq. (5) into Eq. (4) provides the governing differential equation for second grade fluid as:

$$\frac{\partial u}{\partial t} = -\left(\frac{1}{\rho}\right)\left(\frac{\partial p}{\partial x}\right) + \nu\left(\frac{\partial^2 u}{\partial y^2}\right) + \beta\left(\frac{\partial^3 u}{\partial y^2 \partial t}\right) \tag{6}$$

2.2. Solution of present problem with Finite integral transform (FIT) approach

Finite integral transform is a classical exact analytical approach especially suitable for solving higher order mixed partial

derivative. The objective of this approach is to reduce the order of the differential equation and to convert it into an ordinary differential form. After that with the implementation of inverse theorem, the transformed function into original function is obtained. The major advantage of such approach is to handle higher order term which is also difficult to achieve by employing other analytical techniques [21]. From Eq. (6), it is very clear that the second order fluid flow model is 3rd order mixed partial differential equation. The flow condition in the present research work is Generalized Couette flow and the concerned boundary conditions are represented in Fig. 1. The non-dimensional form of Eq. (6) can be written as:

$$\frac{\partial u^*}{\partial \tau} = 2\lambda + \frac{\partial^2 u^*}{\partial y^{*2}} + \varepsilon \frac{\partial^3 u^*}{\partial y^{*2}\,\partial \tau} \tag{7}$$

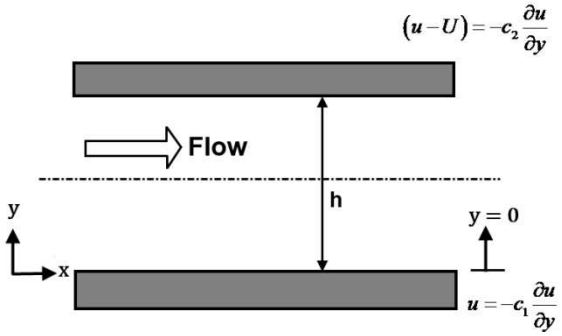

Fig. 1. Schematic diagram of flow regime for present research work

where the non-dimensional parameters are:

$$u^* = u/U;\;\; y^* = y/h;\; \tau = \upsilon t/h^2;\; \varepsilon = \beta U^2/\nu^2;\;\; \lambda = (-dp/dx)h^2/2\mu U \tag{8}$$

The dimensionless boundary conditions are written as follows:

$$\text{at}\;\; y^* = 0\;;\;\; u^* + s_1 \frac{\partial u^*}{\partial y^*} = 0 \qquad \text{for all } \tau \tag{9a}$$

$$\text{at}\;\; y^* = 1\;;\qquad u^* + s_2 \frac{\partial u^*}{\partial y^*} = 0 \qquad \text{for all}\;\; \tau \in [0,1) \tag{9b}$$

The initial condition is:

$$\text{at}\;\; \tau = 0\;;\;\; u^*(y^*) = 0 \tag{9c}$$

To solve Eq. (7) with the above mentioned initial and boundary conditions, we implement the following shift variables first:

$$u^*(y^*,\tau) = \Psi(y^*,\tau) + \Omega(y^*) \tag{10}$$

With the help of Eq. (10), Eq. (7) can be rewritten as:

$$\frac{\partial \Psi}{\partial \tau} = \frac{\partial^2 \Psi}{\partial y^{*2}} + \varepsilon \frac{\partial^3 \Psi}{\partial y^{*2}\,\partial \tau} \tag{11a}$$

and

$$\frac{\partial^2 \Omega}{\partial y^{*2}} + 2\lambda = 0 \tag{11b}$$

The solution of Eq. (11b) is obtained using boundary conditions (9a) and (9b) as follows:

$$\Omega(y^*) = -\lambda y^{*2} + by^* + c \tag{12}$$

where

$$b = \frac{\lambda(1+2s_2)+1}{(s_2 - s_1 + 1)} \quad \text{and} \quad c = -s_1 b \tag{13}$$

Based on Eqs. (10) and (12), the modified form of initial condition as mentioned in Eq. (9c) can be expressed as:

$$\Psi\left(y^*,0\right)=-\Omega\left(y^*\right)=\lambda y^{*2}-by^*-c \tag{14}$$

Now applying the finite integral transform on Eq. (11a) by multiplying Kernel function $K_n(y^*)$ and integrating over the domain of y*, gives:

$$\frac{\partial}{\partial\tau}\int_0^1\Psi\left(y^*,\tau\right)K_n\left(y^*\right)dy^*=\int_0^1\frac{\partial^2\Psi\left(y^*,\tau\right)}{\partial y^{*2}}K_n\left(y^*\right)dy^*+\varepsilon\frac{\partial}{\partial\tau}\int_0^1\frac{\partial^2\Psi\left(y^*,\tau\right)}{\partial y^{*2}}K_n\left(y^*\right)dy^* \tag{15}$$

Implementing boundary conditions (refer Eq. (9a-9b)) on Eq. (15) raises the unknown functions as $\partial\Psi(0,\tau)/\partial y^*$ and $\partial\Psi(1,\tau)/\partial y^*$. To eliminate such functions, Kernel function is considered such that:

$$K_n\left(0\right)+s_1\frac{dK_n\left(0\right)}{dy^*}=0 \tag{16a}$$

and

$$K_n\left(1\right)+s_2\frac{dK_n\left(1\right)}{dy^*}=0 \tag{16b}$$

Assuming the Eigen value problem as follows:

$$\frac{d^2K_n}{dy^{*2}}+\xi_n^2K_n=0 \tag{17}$$

where, ξ_n is the Eigen value of n^{th} order. The solution of Eq. (17) gives:

$$K_n=C_1\cos\left(\xi_n y^*\right)+C_2\sin\left(\xi_n y^*\right) \tag{18}$$

Applying Eqs. (16a) and (16b) simultaneously on Eq. (18) gives:

$$K_n=C'\sin\left(\xi_n y^*-\theta\right) \tag{19}$$

where

$$\tan\left(\xi_n\right)=\frac{\xi_n\left(s_1-s_2\right)}{\left(1+s_1s_2{\xi_n}^2\right)} \tag{20}$$

and

$$\theta=\tan^{-1}\left(s_1\xi_n\right) \tag{21}$$

Now assuming:

$$\int_0^1\Psi\left(y^*,\tau\right)K_n\left(y^*\right)=\int_0^1\Psi\left(y^*,\tau\right)C'\sin\left(\xi_n y^*-\theta\right)=\bar{\Psi}\left(n,\tau\right) \tag{22}$$

And employing Eq. (22) on Eq. (15) gives:

$$\frac{d\bar{\Psi}}{d\tau}=-\xi_n^2\bar{\Psi}-\varepsilon\xi_n^2\frac{d\bar{\Psi}}{d\tau} \tag{23}$$

The solution of Eq. (23) can be given as:

$$\bar{\Psi}\left(n,\tau\right)=A_n\exp\left(-C_n\tau\right) \tag{24}$$

where

$$C_n=\frac{\xi_n^2}{\left(1+\varepsilon\xi_n^2\right)} \tag{25}$$

To find out A_n from Eq. (24), we have employed modified initial condition along with the orthogonal property relation and it asserts:

$$A_n = \left(-\lambda + b + c\right)\cos\left(\xi_n - \theta\right)/\xi_n - c\cos\theta/\xi_n + \left(2\lambda - b\right)\sin\left(\xi_n - \theta\right)/\xi_n^2 - b\sin\theta/\xi_n^2 + 2\lambda\left(\cos\left(\xi_n - \theta\right) - \cos\theta\right)/\xi_n^2 \quad (26)$$

Hence the final solution of unsteady second grade fluid flow can be mathematically presented as:

$$u^*\left(y^*,\tau\right) = \left(-\lambda y^{*2} + by^* + c\right) + 2\sum_{n=1}^{\infty} A_n \exp\left(-C_n\tau\right)\sin\left(\xi_n y^* - \theta\right) \quad (27)$$

Here it may be noted that the ξ_n in Eq. (27) has been found out with the help of the Newton-Raphson iterative method implemented on Eq. (20).

3. Results and Discussion

The solution of the second grade fluid flow model as constructed in the present work (refer Eq. (7)) can be solved by numerical technique also [23]. When both the analytical and numerical solutions exist for a particular governing differential equation, then analytical solution is obviously better as it is considered to be exact and is independent on the size of solution domain. Hence the present analytical solution based on the finite integral transform indicates the superiority of other solution methodologies to handle the higher order mixed partial derivate based governing differential equation.

The first and foremost objective of this research work is to justify the accuracy of the present mathematical modeling with the existing research work. From the literature survey we have found out that Erdoğan and İmrak [8] have developed an analytical solution of governing differential equation of second grade fluid by employing Laplace transform method for the no-slip boundary condition. The present analysis is unsteady in nature and we have employed a finite integral transform method to establish a better analytical model for including both the slip and no-slip circumstances. In Fig. 2a, we have plotted the curve for comprising of average velocity with time for both Newtonian and non-Newtonian fluid in consideration of no-slip boundary ($s_1 = s_2 = 0$). In this context we would like to mention that Erdoğan and İmrak [8] haven't studied flow behavior in transient manner. But we emphasized that the most practical flow behavior is time dependent and we have utilized the solution derived by Erdoğan and İmrak [8] in unsteady form to validate with the present study. First of all it can be clearly notified from Fig. 2a that for both Newtonian ($\varepsilon = 0$) and non-Newtonian ($\varepsilon = 1$) fluid flow, the velocity distribution with the temporal coordinate exactly matches with the published research output. It has been also noticed that the time taken to reach the free stream velocity ($U_{av} = 1$) of the fluid for non-Newtonian fluid is higher than the Newtonian fluid. The physical significance behind such flow behavior is non-linear relation between the viscosity and shear stress induced by unsteady nature of the second grade fluid. In case of Newtonian fluid, shear stress varies linearly with the viscosity and reaches the up-steam velocity (at $\tau = 0.48$) in most convenient manner as portrayed in Fig. 2a. But in case of non-Newtonian flow, non-linear behavior of viscosity combines with unsteady characteristics and takes certain time ($\tau = 4.52$) to reach the up-stream velocity in the flow regime. Hence such graphical justification depicted in Fig. 2a actually authenticates the accurateness of the present research output as well as exactness of the computer codes. On the other hand, for the slip boundary condition, there is no study available in the existing literature to compare the present model. Due to this fact, for the comparison of results for slip boundary conditions, Eq. (7) has been solved numerically using the finite difference method along with the boundary and initial conditions (Eqs. (9a) – (9c)). For the numerical model, the governing equation and the boundary conditions have been discretized by Crank-Nicolson method [24] with second order accuracy to become unconditionally stable and the solution has been made by tridiagonal matrix algorithm. Figure 2b is drawn from the results obtained from the present study and this numerical method and an excellent agreement between these two results is found. Therefore, a correct analytical model in this study for the slip boundary conditions is also established.

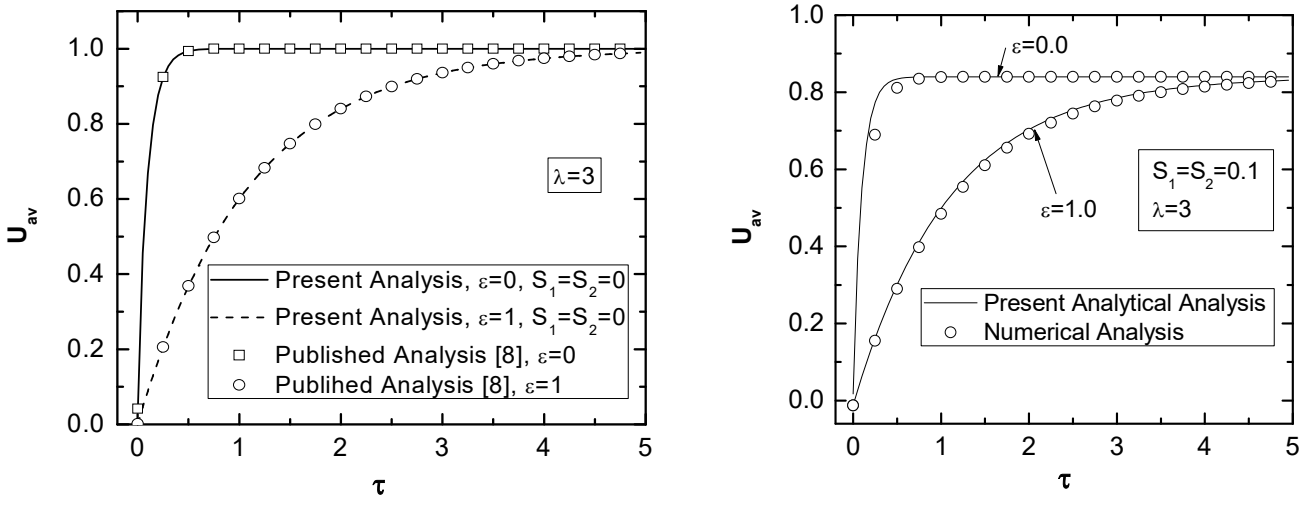

(a): No-slip flow (b): Slip flow

Fig. 2. Validation of the present study for Newtonian and non-Newtonian fluids with no slip and slip velocities at the boundaries.

Our next objective is to study the velocity distribution in the flow regime with the no-slip boundary condition ($s_1 = s_2 = 0$) for different non-dimensional pressure gradients (λ) at a fixed time. From Fig. 3a, at $\tau = 0.1$ a symmetrical velocity distribution with spatial coordinate has been observed for different λ. Basically depending on the magnitude of λ, orientation of velocity changes from the negative to positive slope and for $\lambda = -3$ and $\lambda = +3$, it has been experienced. For all the curves of different λ, starts from zero velocity and meets at particular point of $u^* = 0.62$ and then reaches to a maximum velocity of $u^* = 1$ as a single curve form. We have observed the same trend of velocity distribution with the spatial form for considering $\tau = 1.0$ as depicted in Fig. 3b. But a certain difference has been noticed such as at $\lambda = 0$, slope of velocity curve is exactly linear in comparison with the curve produced in case of $\tau = 0.1$. For other values of λ also the slope of velocity curves are different (more in diffused form) in comparison with Fig. 3a. The major difference has been detected as different curves meet at the point exactly at $u^* = 1$. The importance of unsteady analysis of flow behavior has been greatly understood in such analysis. When time tends to zero i.e. initial condition, the velocity orientation is exactly different than the higher time zone. Hence the unsteady analysis of 2nd grade fluid would be very helpful for the practical investigation of flow behavior.

Figure 4 represents the velocity distribution in flow regime with the slip boundary condition ($s_1 = s_2 = 0.1$) for different non-dimensional pressure gradient (λ) at a fixed time. First of all the variation of velocity with spatial coordinate is exactly same as experienced in Fig. 3. At $\tau = 0.1$ the velocity for different λ coincides at the location of $y^* = 0.12$ (at the vicinity of lower plate). But a certain abruptness of velocity distribution has been detected near the wall of the upper plate (at $y^* = 1$). The velocity of different λ has not been coincided at a particular point (as noted in case of Fig. 3a) but attains in different magnitude such as for $\lambda = -3$; $u^* = 0.37$ and for $\lambda = +3$; $u^* = 0.71$. The probable reason of such behavior would be discontinuity of velocity field in the fluid-solid interface and inhomogeneous thin layer of fluid adjacent to the wall with different rheological properties to the bulk motion of the fluid. The first phenomenon is termed as true slip and latter one is considered as apparent slip. The combination of both actually facilitates the fluid movement nearer to the wall [25]. When a slip occurs before the bulk-yielding while the material is still solid, slipping usually occurs through a very thin boundary layer of the fluid where the stress in this boundary region exceeds the value of yield-stress or through a film from the fluid phase. Figure 4b also exhibits same rheological behaviour at $\tau = 1$ but with different slope of velocity curves. In Fig. 3, for no slip boundary conditions such behaviour hasn't been observed because there is no gliding of fluid layers at the vicinity of the wall boundary and a very specific set of results has been obtained while for Fig. 4 due to influence of hybrid form of true slip and apparent slip, randomness in velocity orientation at the wall surface has been noticed. Hence we firmly recommend incorporating slip boundary condition for non-Newtonian fluid flow analysis.

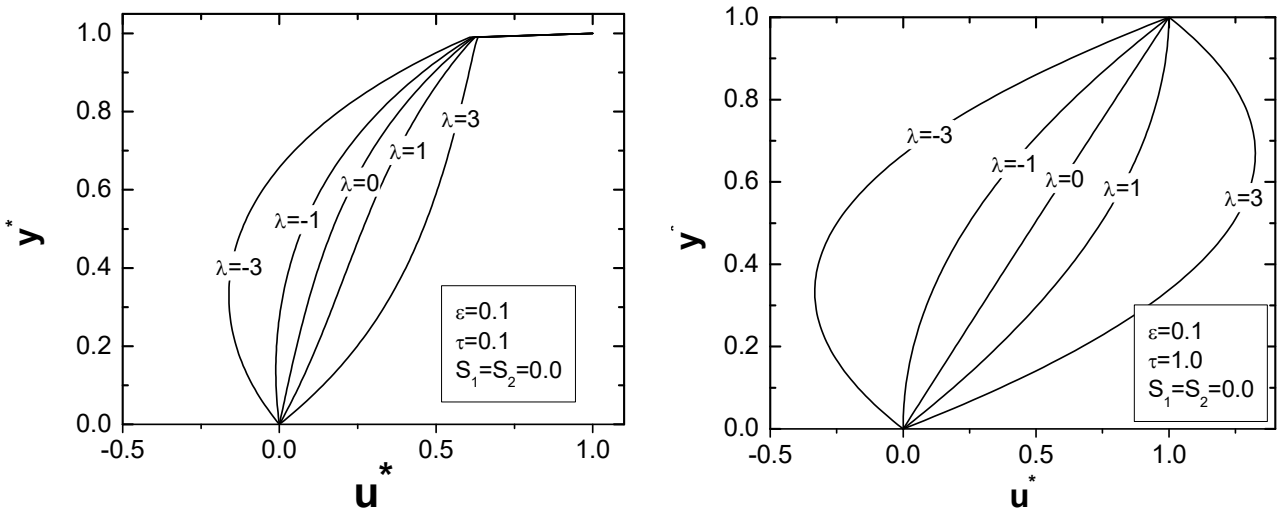

(a): $\tau = 0.1$ (b): $\tau = 1.0$

Fig. 3. Velocity distribution for combined Couette and Poiseuille flow for no slip boundary condition

Figure 5 reveals the research output effect of the pressure gradient on velocity distribution as a function of τ with no slip conditions ($s_1 = s_2 = 0$) for both Newtonian and non-Newtonian fluid. For $\lambda = +3$, we have plotted velocity distribution curves for different τ in the flow regime as scripted in Fig. 5a. It has been observed that larger the τ, higher the tendency of parabolic profile generation. As τ decreases, velocity curve tends to be more flat ($\tau = 0.1$) than higher τ. For both the Newtonian and non-Newtonian fluid, velocity profile exactly matches at $\tau = 5$. The absence of slip at the boundary surface creates a usual boundary layer in the flow field where viscous effects and velocity gradients are substantial. When two layers glide each other, a relative shear force has been generated which actually increases with time of action on the flow. Hence at higher time ranges, parabolic velocity profile has been noticed. In Fig. 5b, we have studied same aspect of flow characteristics at $\lambda = -3$. As the direction of the pressure gradient actually provides the impact on the orientation of velocity profile, it has been noticed that with the increase in τ, velocity profile becomes more parabolic nature but in opposite direction (negative magnitude of velocity) as compared to the analysis reported in Fig. 5a.

The final objective of this research paper is to investigate the effect of pressure gradient on velocity distribution as a function of τ with slip conditions ($s_1 = s_2 = 0.1$) for both Newtonian and non-Newtonian fluid. Figure 6a denotes the velocity profile in the

flow regime at λ = +3 for different τ. The trend of velocity distribution observed in this case is almost the same as Fig. 5a. Here also velocity profile for Newtonian and non-Newtonian fluid at τ = 5 exactly matches. But there are some distinct flow characteristics detected near the two wall surfaces. At the lower plate (the starting location) velocity profiles for different τ are very much abrupt and such flow behaviour hasn't been experienced in case of imposed no-slip condition (refer Fig. 5a). At the vicinity of the lower plate all the velocity curves coincide at the location of y* = 0.11 and the corresponding velocity is u* = 0.075. Such flow feature also hasn't been noted in Fig. 5a. The first and foremost reason of such distinguishable flow characteristics is obviously consideration of slip condition in the mathematical modelling. The slip may affect flow field in different forms such as induction of turbulence, flow instabilities, melt fracture and so on. A large transition slip regime would cause a flow to become more instable near the wall and a strong shear force would be present in the layers adjacent to the wall surface. This phenomenon is actually transformation from shear thinning to shear thickening zone. Apart from these, there would be influence of viscous heating, adsorption, entry/exit effects, viscoelasticity which are the important aspects to be experienced during the slip flow. In Fig. 6b, similar flow features have been noticed but in different magnitude and the direction due to selection of negative pressure gradient (λ = -3) which is very much convenient.

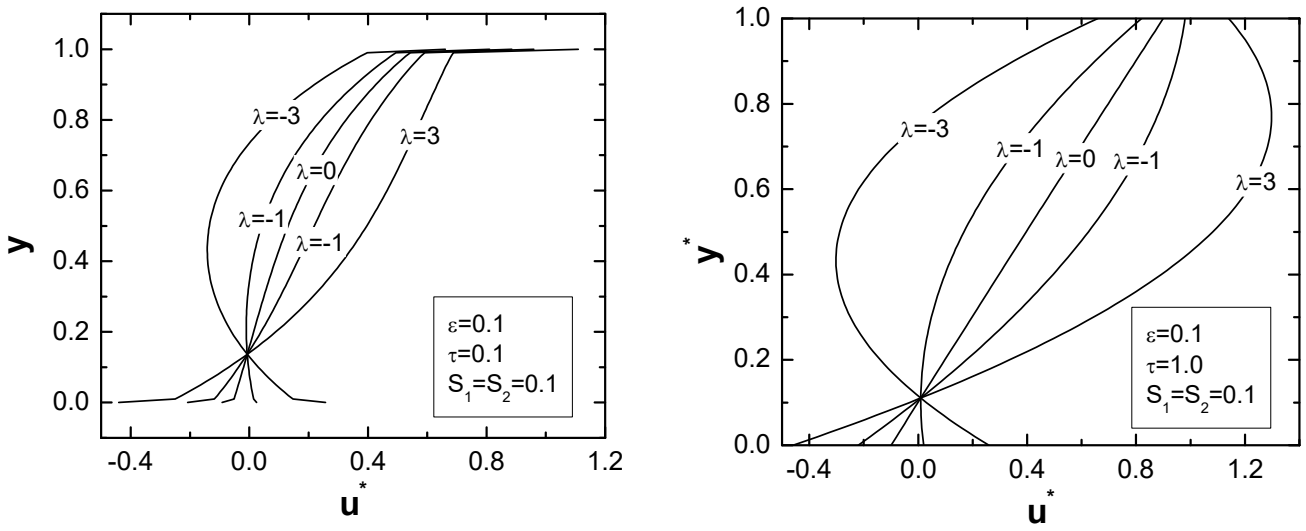

(a): τ = 0.1 (b): τ = 1.0

Fig. 4. Velocity distribution for combined Couette and Poiseuille flow for slip boundary condition

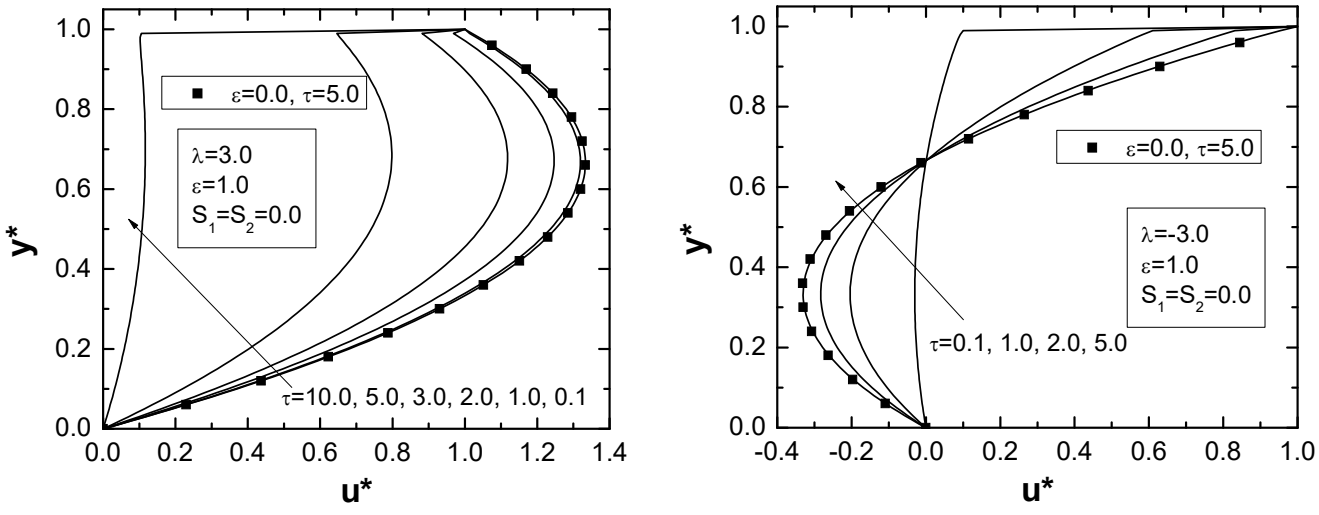

(a): λ = 3.0 (b): λ = -3.0

Fig. 5. Effect of pressure gradient on velocity distribution in combined Couette and Poiseuille flow as a function of τ for no slip conditions

Finally, it can be suggested that during any flow analysis (particularly in microscopic domain), consideration of slip factor must be an anomaly to realize the actual scenario of flow behaviour in the channel. It may also be noted that the present study has considered a second grade fluid but slip conditions must be mandatory for all kind of fluid flow study.

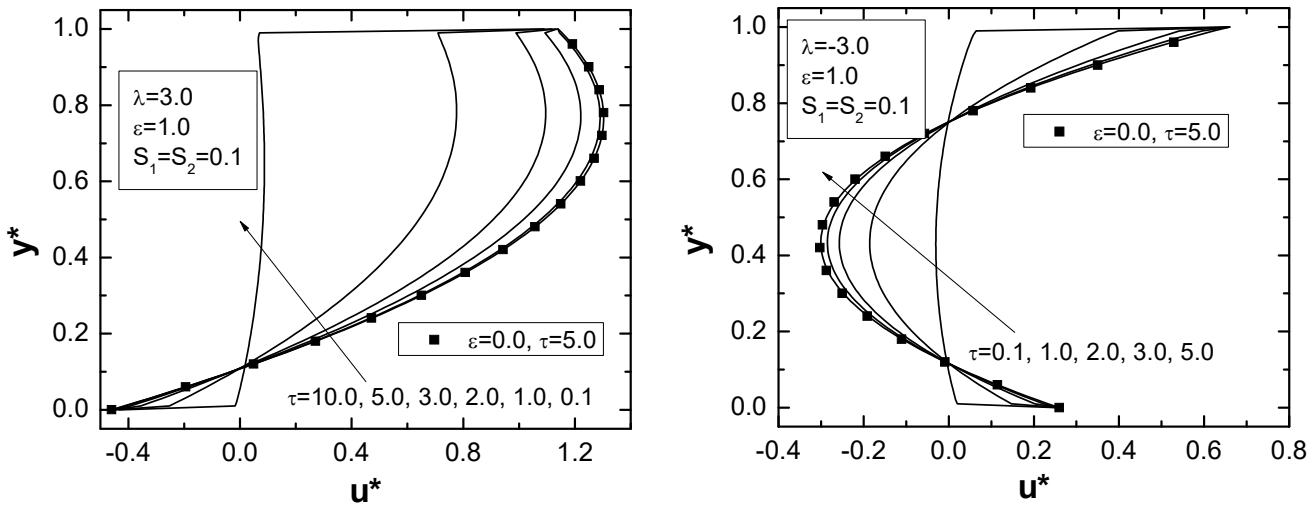

(a): λ = 3.0 (b): λ = -3.0

Fig. 6. Effect of pressure gradient on velocity distribution in combined Couette and poiseuille flow as a function of τ for slip conditions

4. Conclusion

From the present work, following concluding remarks can be outlined:

1) Finite integral transform in conjunction with the separation of variables has been employed to obtain the velocity profile for generalized Couette flow for both Newtonian and non-Newtonian fluid along with slip and no-slip conditions. The validation study of the present work with the published analysis [8] and the developed numerical analysis by Crank-Nicholson scheme has been carried out and it shows well authentication which ensures the correctness of the mathematical modeling and accuracy of computer codes.

2) The impact of non-dimensional pressure gradient *(λ)* for both slip and no-slip conditions has been investigated at a fixed *τ*. A clear distinguishable feature between slip and no-slip condition has been detected. For the slip condition the velocity profile is pretty in organized manner while with no-slip condition the velocity abruptly changes near the wall surface of two plates. The change in direction of *λ* provides the change in direction as well as magnitude of velocity profile in the flow regime.

3) The variation of velocity distribution for different *τ* at a fixed *λ* has been studied and it has been observed that at the boundary, slip flow is random than no-slip condition. The gliding of layer and the non-uniform shear stress generation due to solid-fluid interaction between wall and fluid flowing near it, causes an uneven velocity distribution in comparison with the no-slip condition.

Conflict of Interest

The authors declared no potential conflicts of interest with respect to the research, authorship and publication of this article.

Funding

The authors received no financial support for the research, authorship and publication of this article.

Nomenclature

b, c	Non-dimensional slip constants, refer Eq. (13)	x	Spatial coordinate along longitudinal direction from the lower plate (m), refer Fig. 1
c_1, c_2	Slip constants, see Fig. 1	y*	Non-dimensional spatial coordinate, check Eq. (8)
C_n	Constant as function of Eigen value, check Eq. (25)	α_1, β	Material module, see Eq. (5)
h	Height of the channel, see Fig. 1 [m]	ρ	Density of the fluid, refer Eq. (4) [kg m^{-3}]
I	Directional constant, scripted in Eq. (2)	μ	Dynamic viscosity, see Eq. (5) [N s m^{-2}]
K_n	Kernel function, refer Eq. (15)	ν	Kinematic viscosity (Stokes), refer to Eq. (6)
p	Pressure induced in the flow, check Eq. (1) [Nm^{-2}]	σ_{xy}	Stress developed in the fluid, check Eq. (5) [Nm^{-2}]
s_1, s_2	Induced non-dimensional slip in flow velocity, see Eqs. (9a) – (9b)	τ	Time constant, see Eq. (8)
t	Flow time imposed in the channel, refer Eq. (6) [s]	ε	Non-dimensional viscous term, refer Eq. (8)
u	Unidirectional flow velocity of lower plate, see Fig. 1 [ms^{-1}]	λ	Non-dimensional pressure gradient on flow, refer to Eq. (8)
U	Velocity of the upper plate, see Fig. 1 [ms^{-1}]	Ψ, Ω	Functions utilized for shift of variables, see Eq. (10)
u*	Non-dimensional velocity, check Eq. (8)	ξ_n	Eigen value of nth order, check Eq. (17)
y	Spatial coordinate along vertical direction from the lower plate, refer Fig. 1 [m]		

References

[1] Rajagopal, K.R., Kaloni, P.L., *Continuum Mechanics and its Applications,* Hemisphere Press, Washington, 1989.
[2] Batchelor, G.K., *An Introduction to Fluid Dynamics, Cambridge*, UK, 1967.
[3] Denn, M.M., Extrusion instabilities and wall slip, *Annual Reviews of Fluid Mechanics*, 33(1), 2001, 265–287.
[4] Potente, H., Ridder, H., Cunha, R.V., Global concept for describing and investigation of wall slip effects in the extrusion process, *Macromolecular Materials and Engineering*, 287(11), 2002, 836–842.
[5] Mitsoulis, E., Kazatchkov, I.B., Hatzikiriakos, S.G., The effect of slip in the flow of a branched PP melt: experiments and simulations, *Rheologica Acta*, 44(4), 2005, 418–426.
[6] Ellahi, R., Effects of the slip boundary condition on non-Newtonian flows in a channel, *Communications in Nonlinear Science and Numerical Simulations*, 14(4), 2009, 1377–1384.
[7] Yang, S.P., Zhu, K.Q., Analytical solutions for squeeze flow of Bingham fluid with Navier slip condition, *Journal of Non-Newtonian Fluid Mechanics*, 138(2), 2006, 173–180.
[8] Erdoğan, M.E., İmrak, C.E., On some unsteady flows of a non-Newtonian fluid, *Applied Mathematical Modelling*, 31, 2007, 170–180.
[9] Wu, Y.H., Wiwatanapataphee, B., Hu, M.B., Pressure driven transient flows of Newtonian fluids through microtubes with slip boundary, *Physica A: Statistical Mechanics and Its Applications*, 387(24), 2008, 5979–5990.
[10] Chen, Y.L., Zhu, K.Q., Couette-Poiseuille flow of Bingham fluids between two porous parallel plates with slip conditions, *Journal of Non-Newtonian Fluid Mechanics*, 153(1), 2008, 1–11.
[11] Chatzimina, M., Georgiou, G., Housiadas, K., Hatzikiriakos, S.G., Stability of the annular Poiseuille flow of a Newtonian liquid with slip along the walls, *Journal of Non Newtonian Fluid Mechanics*, 159(1), 2009, 1–9.
[12] Ellahi, R., Hayat, T., Mahomed, F.M., Zeeshan, A., Fundamental flows with nonlinear slip conditions: exact solutions, *Zeitschrift fur Angewandte Mathematik und Physik*, 61(5), 2010, 877–888.
[13] Hady, F.M., Ibrahim, F.S., Abdel-Gaied, S.M., Eid, M.R., Influence of yield stress on free convective boundary-layer flow of a non-Newtonian nanofluid past a vertical plate in a porous medium, *Journal of Mechanical Science and Technology*, 25(8), 2011, 2043–2050.
[14] Svetlana, I.N., Clinton, P.C., The role of Poiseuille flow in creating depth-variation of asthenospheric shear, *Geophysical Journal International*, 190(3), 2012, 1297–1310.
[15] Jeong, N., Rarefied gas flow simulations with TMAC in the slip and the transition flow regime using the lattice Boltzmann method, *Journal of Mechanical Science and Technology*, 28(11), 2014, 4705–4715.
[16] Noor, N.F.M., Haq, R.U., Nadeem, S., Hashim, I., Mixed convection stagnation flow of micropolar nanofluid along a vertically stretching surface with slip effects, *Meccanica*, 50, 2015, 2007–2022.
[17] Sankar, D.S., Lee, U., Influence of slip velocity in Herschel -Bulkley fluid flow between parallel plates - A mathematical study, *Journal of Mechanical Science and Technology*, 30(7), 2016, 3203–3218.
[18] Wang, X., Qi, H., Yu, B., Xiong, Z., Xu, H., Analytical and numerical study of electroosmotic slip flows of fractional second grade fluids, *Communications in Nonlinear Science and Numerical Simulation*, 50, 2017, 77–87.
[19] Ramesh, K., Sharma, T., Effectiveness of radiation and Joule heating on hydromagnetic Carreau fluid through microfluidic channels with slip boundary conditions, *Microsystem Technologies*, 24(12), 2018, 4921–4932.
[20] Dunn, J.E., Fosdick, R.L., Thermodynamics, stability and boundedness of fluids of complexity and fluids of second grade, *Archive for Rational Mechanics and Analysis*, 56, 1974, 191–252.
[21] Hahn, D.W., Ozisik, M.N., *Heat Conduction*, Inc. New Jersey: John Wiley & Sons, 2012.
[22] Rajagopal, K.R., Kaloni, P.L., *Continuum Mechanics and its Applications*, Washington, DC: Hemisphere Press, 1989.
[23] Ye, W.-B., Design method and modeling verification for the uniform air flow distribution in the duct ventilation, *Applied Thermal Engineering*, 110, 2017, 573–583.
[24] Chung T.J., *Computational Fluid Dynamics*, Cambridge University Press, Cambridge, UK, 2002.
[25] Kiljanński, T., A method for correction of the wall-slip effect in a Couette rheometer, *Rheologica Acta*, 28(1), 1989, 61–64.